Detecting nonlinear dynamics of functional connectivity

Stephen LaConte[a1], Scott Peltier[a], Yasser Kadah[a], Shing-Chung Ngan[b], Gopikrishna Deshpande[a], Xiaoping Hu[a]

[a]Department of Biomedical Engineering, Emory University/Georgia Tech, Atlanta, GA USA 30322
[b]Department of Microbiology, University of Washington, Seattle, WA USA 98195

ABSTRACT

Functional magnetic resonance imaging (fMRI) is a technique that is sensitive to correlates of neuronal activity. The application of fMRI to measure functional connectivity of related brain regions across hemispheres (e.g. left and right motor cortices) has great potential for revealing fundamental physiological brain processes. Primarily, functional connectivity has been characterized by linear correlations in resting-state data, which may not provide a complete description of its temporal properties. In this work, we broaden the measure of functional connectivity to study not only linear correlations, but also those arising from deterministic, non-linear dynamics. Here the delta-epsilon approach is extended and applied to fMRI time series. The method of delays is used to reconstruct the joint system defined by a reference pixel and a candidate pixel. The crux of this technique relies on determining whether the candidate pixel provides additional information concerning the time evolution of the reference. As in many correlation-based connectivity studies, we fix the reference pixel. Every brain location is then used as a candidate pixel to estimate the spatial pattern of deterministic coupling with the reference. Our results indicate that measured connectivity is often emphasized in the motor cortex contra-lateral to the reference pixel, demonstrating the suitability of this approach for functional connectivity studies. In addition, discrepancies with traditional correlation analysis provide initial evidence for non-linear dynamical properties of resting-state fMRI data. Consequently, the non-linear characterization provided from our approach may provide a more complete description of the underlying physiology and brain function measured by this type of data.

Keywords: magnetic resonance imaging, functional imaging, functional connectivity, nonlinear dynamics, correlation analysis

1. INTRODUCTION

Functional magnetic resonance imaging (fMRI) is a technique that is sensitive to correlates of neuronal activity, and is often used to obtain localized maps of brain function corresponding to a controlled psychological experiment. Connectivity studies, however, aim to understand the brain as a distributed system and are important for exploring brain function and physiology. Within functional neuroimaging, functional connectivity has been characterized through spatiotemporal correlations between spatially distinct regions of the brain[1,2]. Biswal et al. used the low frequency (< 0.1 Hz) component of baseline (or resting state) data to demonstrate that the left and right motor cortexes were correlated[3]. Lowe[4] subsequently expanded this work, finding correlations to the motor cortex, visual cortex, and amygdala using slower acquisition rates. Here we will use the motor cortex as an example since it is convenient to study in terms of experimental ease and anatomic separation.

Primarily, functional connectivity has been characterized by linear correlations in resting-state data, which may not provide a complete description of its temporal properties. In this work, we broaden the measure of functional connectivity to study not only linear correlations, but also more general deterministic coupling arising from both linear and non-linear dynamics. We are encouraged by the fact that the field of nonlinear dynamics has made large contributions to the characterization of many biologically derived signals such as EEG, ECG, and respiratory movement[5-11]. The goal of these studies is often to evaluate evidence for low dimensional chaotic behavior in distinction from a stochastic model. Commonly, this is done by evaluating the system in terms of predictability or invariant

---

[1] E-mail: slaconte@bme.emory.edu

features (e.g., correlation dimension or Lyapunov exponents)[12]. These approaches rely on reconstructing the dynamical system from multiple independent measures or, more commonly, from a single measured time series. Such studies are particularly challenging in fMRI since we typically work with relatively short and noisy time series. Furthermore, the computational load of these studies, the number of algorithmic free parameters, and the large quantity of spatial locations make traditional measures such as correlation dimension and Lyapunov exponents extremely challenging. Still, one recent study was successful in generating multivariate ensemble estimates of the correlation dimension across tasks of varying complexity[13].

Here, we examine the potential utility of a nonlinear dynamics technique in characterizing functional connectivity. We do so using a bivariate implementation of the delta-epsilon method[11,12], which, in contrast to most nonlinear methods, has the conservative goal of obtaining evidence for determinism rather than a complete characterization of the underlying dynamical system. The general approach is to distinguish deterministically coupled resting state fluctuations from random fluctuations. Here, an extension of the delta-epsilon approach is applied to fMRI data to evaluate whether a time course of a candidate pixel provides additional information concerning the time evolution of a reference pixel time series. As in many correlation-based connectivity studies, a fixed reference pixel is used. Every brain location is then used as a candidate pixel to estimate the spatial pattern of deterministic coupling with the reference.

An important consideration for this work is the issue of physiological noise in fMRI, which arises from cardiac pulsation, respiratory movements, and vasomotor activity. These noise contributions are important because their strength is often comparable to that of the BOLD response. Spectral analysis of fMRI time series has implicated respiratory and cardiac frequencies as the largest contributors to the signal, with complicated and spatially varying contributions[14-16]. Hu et al.[14] have proposed a retrospective technique in which cardiac and respiratory effects are recorded during the fMRI experiment and later linearly regressed out of the data. Biswal and Mitra have focused on frequency domain filtering techniques[15,16]. Somewhat more elusive has been the contribution by vasodilation. This effect seems to contribute power at the 0.1 Hz range[15,16] however the strength and bandwidth is not consistent over space or time. Here we have not considered the delta-epsilon approach on physiologically corrected or otherwise corrected data. This is a complicated issue in nonlinear dynamics studies[17]. We do however begin to address the issue of physiological noise by using cardiac and respiration signals as embedding references in addition to jointly embedding these signals with a motor seed pixel.

2. THEORY

The delta-epsilon approach was developed to study non-linear dynamical systems from short, low SNR time series[11,12], which are desirable properties for fMRI analysis. Here we use the bivariate formulation of the delta-epsilon technique[11] to examine deterministic coupling between a fixed time series and multiple "candidate" time series consisting of all measured brain locations. This technique relies on determining whether the candidate pixel provides additional information concerning the time evolution of the reference. We independently considered three signals as the fixed reference. Primarily we used a "seed" pixel from the motor cortex. This is analogous to conventional, correlation-based functional connectivity studies. In addition we examined cardiac and respiration signals as fixed. Further we have examined the multivariate embedding of seed, cardiac, and respiration as a reference to examine the joint system's coupling to each candidate pixel time series. In the following subsections, we discuss the various components of the bivariate delta-epsilon technique, including generation of an appropriate image representation of results.

2.1. Phase-space reconstruction

The method of delays is used to reconstruct the joint system defined by a reference time series x(t) and a candidate pixel time series y(t). The joint phase space is,

$$Q(t) = \{x(t), x(t-\tau), x(t-2\tau), \ldots, x(t-(m-1)\tau), y(t), \ldots, y(t-(n-1)\tau)\}, \tag{1}$$

where m and n are the respective embedding dimensions of $x(t)$ and $y(t)$, and the joint space has dimension $m+n$. Note that in this bivariate case (and in general multivariate extensions) this is a hybrid approach between pure reconstruction using delays and pure reconstruction using multiple independent measurements. See Cao[18], Abraham[19], Albano[20] for different perspectives on the phase-space reconstruction problem.

2.2. Delta-epsilon calculation

Within the phase space, the delta-epsilon method looks at pairs of times (pre-images) and their future states (images). As an example for $m=n=2$, we would consider the phase space points $\{x(t_i),x(t_i-\tau),y(t_i),y(t_i-\tau)\}$ and $\{x(t_j),x(t_j-\tau),y(t_j),y(t_j-\tau)\}$ with their images $x(t_{i+1})$ *and* $x(t_{j+1})$ for times i and j respectively. If the system has deterministic properties, we would expect small distances between pre-images (δ) to result in small average distances between images (ε).

2.3. Surrogate data and significance

To obtain estimates of significance, we generate surrogate data by randomly permuting the $y(t)$ contribution to the phase space (keeping coordinates together, but randomizing their temporal order). We obtain a statistic,

$$S(r) = \frac{\left|\varepsilon(r) - \varepsilon^*(r)\right|}{\sigma^*(r)} \, , \tag{2}$$

where $\varepsilon^*(r)$ and $\sigma^*(r)$ are average image distance and standard deviation of the surrogate data, respectively. As described by Kaplan[12], we use a cumulative ε as the average image distances for $\delta < r$.

2.4. Bivariate mapping procedure

For our application we fix $x(t)$ and obtain $S(r)$ estimates for every brain location. To display results as an image, the $S(r)$ for each pixel must be reduced to a single statistic. We considered taking the mean and max of $S(r)$, and found maps generated by calculating the mean. In addition, restricting consideration to $r_{min} < r < r_{max}$ was found to be beneficial.

3. METHODOLOGY

The general goals of this study were to i) assess the appropriateness of the bivariate delta-epsilon method for resting state connectivity studies, ii) look for discrepancies between linear correlation methods and the delta-epsilon method, and iii) evaluate the contribution of physiologic noise to the bivariate delta-epsilon technique. Common to the methodologies examining each of these issues was that a fixed time series was jointly embedded with the time series of each individual brain pixel, giving a pixel-specific assessment of delta-epsilon coupling. In this case, the fixed time series was either a seed pixel from the data itself, or an external measurement of hear-beat or respiration. Seed pixels were chosen from a separate motor experiment performed during the same imaging session, as is commonly done in conventional cross-correlation based functional connectivity studies.

3.1. Suitability for functional connectivity

Two oblique, axial, EPI slices through the primary motor cortex were imaged. Resting state data were collected from a single subject for eight minutes on a 3T Siemens Magnetom Trio (TR/TE = 200/32 ms, voxel size=3.4×3.4×5 mm^3). The subject then performed a sequential finger opposition task performing 20 s each of left-hand, right-hand, and rest. This series was repeated 4 times (for a total of 4 min.), using the same parameters image acquisition parameters. For the finger opposition data, a *t*-test of right hand vs. rest was performed to obtain a reference pixel. This location became the $x(t)$ for the delta-epsilon method, which was performed on the resting state data using $m=n=2$, and τ set to 10 time samples, corresponding to the first minimum of the autocorrelation function of $x(t)$.

3.2. Discrepancies between linear correlation and delta-epsilon

Resting state data consisted of nine axial, EPI slices, ranging from the top of the head to the base of the corpus callosum in a single subject on a 3T Siemens Magnetom Trio (TR/TE = 750/35 m, slice gap = 7.5 mm voxel size=3.4×3.4×5 mm^3), giving 1024 time measurements in 12.8 min. The slice showing the best motor activation pattern from a separate bimanual finger opposition task, was chosen for our study. A seed pixel was also obtained from the motor task. For the delta-epsilon method, the initial 10 images were discarded, $m=n=2$, $\tau=1$.

3.3. Contribution of physiologic noise

Resting state data consisted of five axial, EPI slices, ranging from the top of the head to just above the corpus callosum on a 3T Siemens Trio (TR/TE = 750/35 ms, slice gap = 5 mm voxel size=3.4×3.4×5 mm^3), giving 1120 time measurements in 14 min. The slice showing the best motor activation pattern from a separate bimanual finger opposition task, was chosen for our study. A seed pixel was also obtained from the motor task. For the delta-epsilon method, the initial 10 images were discarded, $m=n=2$, $\tau = 1$. During the fMRI scanning session, the subjects' respiratory and cardiac rhythms were recorded using a physiological monitoring unit (In Vivo Research, Orlando, FL) connected to a data acquisition board. In-house code sampled the physiological rhythms at a sampling rate of 200 Hz, triggered by the start of the MRI scans. This experiment was repeated in two subjects. Since the sampling time for the fMRI data is 750 ms (i.e., sampling frequency = 4/3 Hz), rapid heart rate and respiration will be present in an aliased form within the fMRI signals. To account for this aliasing effect, physiologic recordings were downsampled to the fMRI acquisition rate, without prior low-pass filtering[14,15].

4. RESULTS

The right motor pixels from the finger opposition task are shown in Fig. 2(a). One of these pixels was chosen as the reference pixel, and the results of the delta-epsilon method in the resting task are also shown in Fig. 2(a). Fig. 2(b) shows $S(r)$ for the seed pixel and from the delta-epsilon results in Fig. 2(a). Note that the delta-epsilon method was performed at every spatial location, but the left motor region (surrounding the reference pixel) has lower significance results than the right motor region (see Fig 2C). One explanation is the fact that the reference pixel, when combined with itself, adds no addition predictive information. It follows that pixels in its neighborhood may also exhibit similarities to the reference that they too contribute little extra information.

Figure 3 shows an example of a pattern emerging from a delta-epsilon result where none is present in the corresponding correlation analysis. Unfortunately, physiological signals were not collected for these data. Looking at the power spectrum, however, illustrates a relatively flat spectrum, perhaps colored by physiology at 0.2 Hz. This is a prime example of data that appear to represent noise from the perspective of traditional linear analysis that nonetheless demonstrate deterministic properties. We want to avoid over-interpreting this result, though. Currently we are searching for a systematic means of discovering other such time series.

Figures 4, 5, and 6 illustrate results for subject 1 in the study of physiological noise. In Fig. 4, the results show some similarity between seed pixel delta-epsilon and cross-correlation results. For the cardiac delta-epsilon result, few pixels show significance, but those that do tend to fall, plausibly, along the midline. No corresponding pattern is found for the cardiac correlation map. For respiration, the delta-epsilon pattern looks surprisingly similar to the seed pixel pattern. For the correlation map, pixels along the edges tend to be most affected. This correlation pattern corresponds well to results in the literature (e.g. Kruger[21]). The power spectra of each of the three reference time series are shown in Fig. 5. All three have the greatest proportion of their power centered at 0.1 Hz or lower. Thus cardiac and respiration contributions for this subject are overlapping the low frequency spectral bands, which would normally be attributed to resting state connectivity. Finally Fig. 6 shows the result of jointly embedding the motor seed pixel, cardiac, and respiration as the delta-epsilon reference. The result looks very similar to the respiration map in Fig. 4, with perhaps the addition of the supplemental motor area in the center region.

Figures 7, 8, and 9 correspond to Figs. 4, 5, and 6, but for subject 2. In this case the dominant frequencies for the down-sampled physiologic signals are distinct from the motor seed pixel as well as from themselves (Fig. 8). There is also good correspondence between delta-epsilon maps and correlation maps in Fig. 7. Cardiac maps show a large amount of agreement, even though, correlation values are very low and delta-epsilon significances are reasonably high. For this subject, there seems to be little contribution from the respiration signal. The results for subject 2 differ from subject 1 in that the seed pixel map is relatively clean, while the respiration map is noisy with very low average significance levels. The joint embedding of seed and physiology, though, produces a noisy, low-significance map. It is surprising that this does not produce some combination of the stronger seed or cardiac maps as in subject 1. One explanation for this may be the delta-epsilon algorithm's reliance on exceptional events (relying on close distances in the phase space); the inclusion of the apparently weak and noisy respiration information may increase distances in the phase space, decreasing our chance of observing such fine detail. This issue needs to be explored further.

One possible outcome of jointly embedding the seed pixel time series and physiological signals is that contra-lateral connectivity could be examined while simultaneously suppressing contributions from physiology. This is based on the observations in Fig. 2 that seed pixels tend to have lower delta-epsilon results. Although we have obtained very different results in Figs. 6 and 9, both seem to illustrate that this joint embedding approach, by itself is not well suited to improving measures of resting state connectivity (by suppressing physiologic artifacts). For this to work, the contribution of these effects would have to be spatially and temporally uniform in their contribution to the pixel dynamics. Our results, however, give encouraging evidence for using this as a tool to examine physiology and point to the feasibility of correcting for physiology based on nonlinear dynamics prediction techniques on a pixel-by-pixel basis.

The results from subjects 1 and 2 indicate that there is, in general, a fair amount of similarity between correlation maps and delta-epsilon maps (using a motor seed pixel). The differences in the results, however, are the most intriguing aspect of this work in that they give evidence for the strengths and shortcomings of each approach. If a pixel is detected through correlation analysis, and not in delta-epsilon procedure, this could mean that SNR was too poor, too few time samples were acquired, the parameters leading to the joint embedding were sub-optimal, or that the surrogate data and statistical test were inappropriate or lacked power. In cases where pixels are found via delta-epsilon that are not explained by linear correlation, we have good candidates for pursuing further characterization in terms of non-linear dynamics. An example of this is illustrated in Fig. 3, where a structured map is produced by the delta-epsilon approach using a time series that, through spectral analysis and cross correlation techniques appears to be highly noisy.

5. CONCLUSIONS

A new approach to analyzing functional connectivity data based on nonlinear dynamical modeling is presented. The new method complements the conventional correlation analysis and provides an insight to aspects of the process that are valuable to better understanding of the underlying processes. Our results indicate that bilateral connectivity results can be obtained, often emphasizing the motor cortex contra-lateral to the reference pixel, demonstrating the appropriateness of this approach for functional connectivity studies. In addition, discrepancies with traditional correlation analysis provide initial evidence for non-linear dynamical properties of resting-state fMRI data. Thus the non-linear characterization provided from our approach may provide a more complete description of the underlying physiology and brain function measured by this type of data. Finally the bivariate delta-epsilon technique was able to show coupling between physiological signals and fMRI data.

Further work is needed to examine several issues including the dependence on TR and number of samples, which affect SNR and experiment duration. We are also examining disciplined methods for constructing the joint, hybrid phase space in terms of τ and embedding dimensions. Further, it should be possible to avoid the use of surrogate data estimates for each candidate pixel by instead using the distribution of results from all brain locations. Finally more subjects, of various basal cardiac and respiration levels are needed to study physiological effects presented here.

ACKNOWLEDGEMENTS

REFERENCES

1. S. C. Strother, J. R. Anderson, K. A. Schaper, J. J. Sidtis, J.-S. Liow, R. P. Woods, and D. A. Rottenberg, "Principal component analysis and the scaled subprofile model compared to intersubject averaging and statistical parametric mapping. I. "Functional Connectivity" of the human motor system studied with [15O]water PET," *J Cereb Blood Flow Metab* **15**, pp. 738-753, 1995.
2. K. J. Friston, C. D. Frith, P. F. Liddle, and R. S. J. Frackowiak, "Functional connectivity: The principal component analysis of large (PET) data sets," *J Cereb Blood Flow Metab* **13**, pp. 153-171, 1993.

3. B. Biswal, F. Z. Yetkin, V. M. Haughton, and J. S. Hyde, "Functional connectivity in the motor cortex of resting human brain using echo-planar MRI," *Magn Res Med* **34**, pp. 537-541, 1995.

4. M. J. Lowe, B. J. Mock, and J. A. Sorenson, "Functional connectivity in single and multislice echoplanar imaging using resting-state fluctuations," *NeuroImage* **7**, pp. 119-132, 1998.

5. W. S. Pritchard and D. W. Duke, "Measuring chaos in the brain: A tutorial review of nonlinear dynamical EEG analysis," *Intern J Neuroscience* **67**, pp. 31-80, 1992.

6. K. Narayanan, R. B. Govindan, and M. S. Gopinathan, "Unstable periodic orbits in human cardiac rhythms," *Phys Rev E* **57**, pp. 4594-4603, 1998.

7. O. Fojt and J. Holcik, "Applying nonlinear dynamics to ECG signal processing," *IEEE Eng Med Biol* **17**, pp. 96-101, 1998.

8. T. Elbert, B. Rockstroh, Z. J. Kowalik, M. Hoke, M. Molnar, J. E. Skinner, and N. Birbaumer, "Chaotic brain activity," *EEG* **Suppl. 44**, pp. 441-449, 1995.

9. N. Pradhan, P. K. Sadasivan, S. Chatterji, and D. N. Dutt, "Patterns of attractor dimensions of sleep EEG," *Comput Biol Med* **25**, pp. 455-462, 1995.

10. M. Kobayashi and T. Musha, "1/f fluctuation of heartbeat period," *IEEE Trans Biomed Engr*, **29**, pp. 456-457, 1982.

11. D. Hoyer, D. Kaplan, S. Friedrich, and M. Eiselt, "Determinism in bivariate cardiorespiratory phase-space sets," *IEEE Eng Med Biol* **17**, pp. 26-31, 1998.

12. D. Kaplan, "Exceptional events as evidence for determinism," *Physica D* **73**, pp. 38-48, 1994.

13. M. Dhamala, G. Pagnoni, K. Wiesenfeld, and G.S. Berns, "Measurements of brain activity complexity for varying mental loads," *Physical Review E* **65**:041917, 2002.

14. X. Hu, T. H. Le, T. Parrish, and P. Erhard, "Retrospective estimation and correction of physiological fluctuation in functional MRI," *Magn Reson Med* **34**, pp. 201-212, 1995.

15. B. Biswal, E. A. DeYoe, and J. S. Hyde, "Reduction of physiological fluctuations in fMRI using digital filters," *Magn Reson Med* **35**, pp. 107-113, 1996.

16. P. P. Mitra, S. Ogawa, X. Hu, and K. Ugurbil, "The nature of spatio-temporal changes in cerebral hemodynamics as manifested in functional magnetic resonance imaging," *Magn Reson Med* **37**, pp. 511-518, 1997.

17. J. Theiler, B. Galdrikian, A. Longtin, S. Eubank, and J.D. Farmer, "Using surrogate data to detect nonlinearity in time series," Casdagli, M. and Eubank, S. editors. In *Nonlinear Prediction and Forecasting* (Addison-Wesley, 1991).

18. L.Y. Cao, "Practical method for determining the minimum embedding dimension of a scalar time series," *Physica D* **110**, pp. 43-50, 1997.

19. F.D. Abraham, "Nonlinear coherence in multivariate research: Invariants and the reconstruction of attractors. Nonlinear Dynamics," *Psychology, and Life Sciences* **1**, pp. 7-33, 1997.

20. A.M. Albano, J. Muench, and C. Schwartz, "Singular value decomposition and the Grassberger-Procaccia algorithm," *Phys. Rev. A* **38A**, pp. 3017-3026, 1988.

21. G. Kruger, and G. H. Glover, "Physiological noise in oxygenation-sensitive magnetic resonance imaging," *Magn Reson Med* **46**, pp. 631-637, 2001.

Pseudocode

```
x=getSeedPixel();
foreach y=1:n_brainLoc {
        phaseSpace=constructPS(x,y);
        de = δ-ε(phaseSpace);
        foreach i=1:N {
                surrogatePS=surPhaseSpace(de);
                s_de[i]= δ-ε(surrogatePS);
        }
        S=compare(de,s_de);
        //(mean significance across radius)
        deMap(brainLoc)=mean(S);
}
```

$$S(r) = \frac{\left|\varepsilon(r) - \varepsilon^*(r)\right|}{\sigma^*(r)}$$

$\varepsilon^*(r)$ average image distance
$\sigma^*(r)$ standard deviation of surrogate data

Fig. 1. Pseudo code for bivariate delta-epsilon functional connectivity studies.

Task Result

Delta-Epsilon Result

Significance vs. Pre-Image Distance
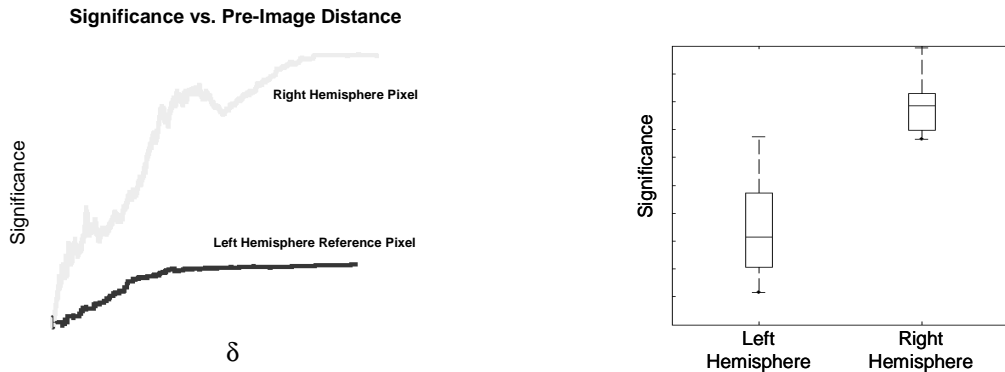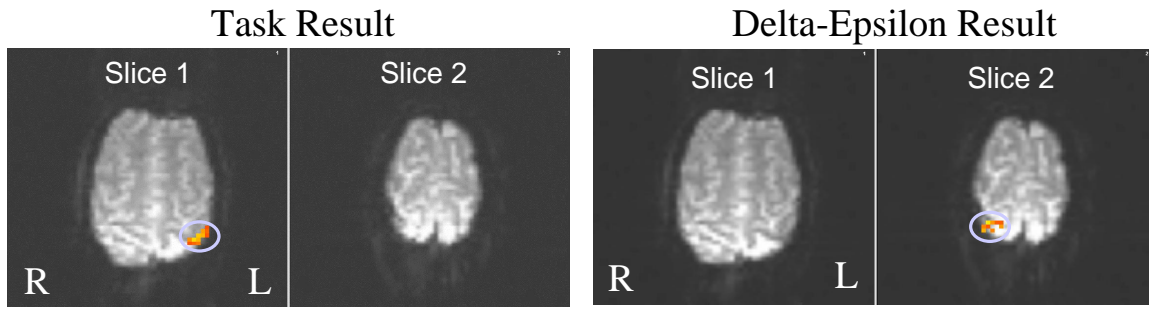
Fig. 2. Demonstration of delta-epsilon and significance estimates from surrogate data.

delta-epsilon

cross correlation
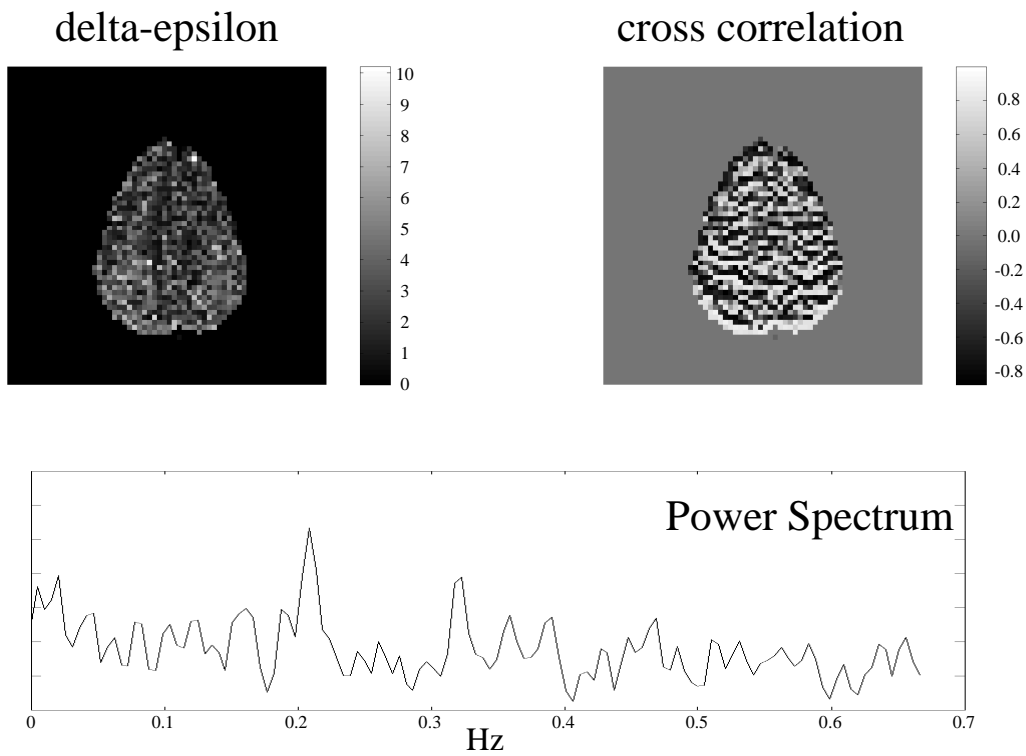
Power Spectrum

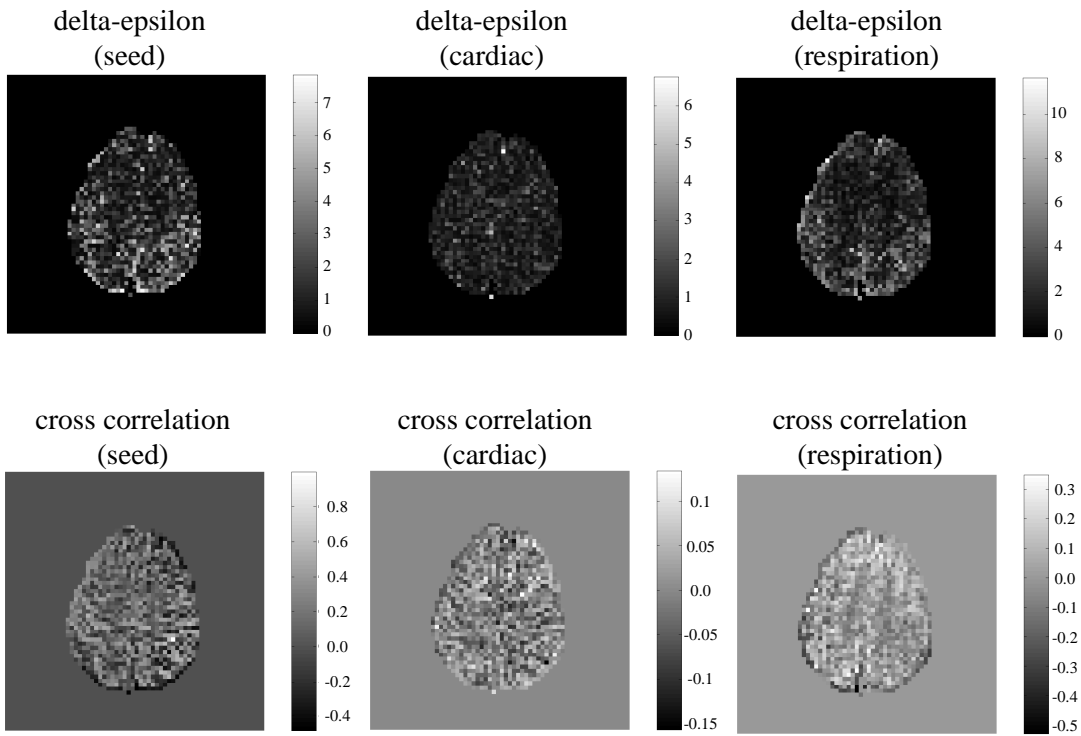Fig. 3. Discrepancies between linear correlation and delta-epsilon.

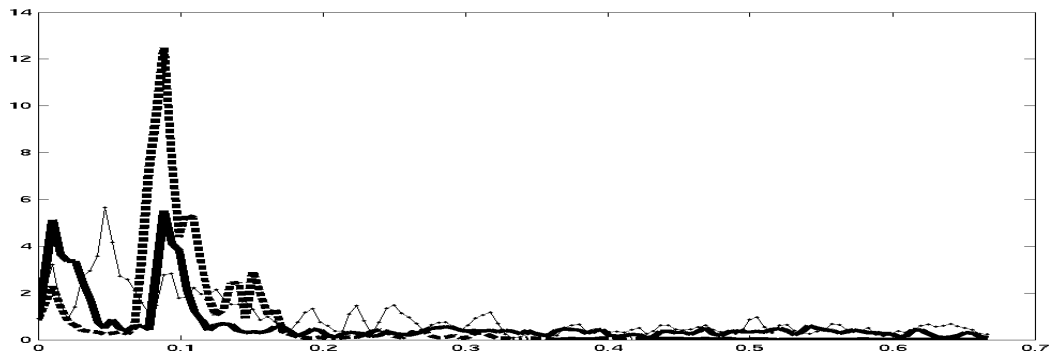Fig. 4. de and correlation results using seed pixel, downsampled cardiac data and downsampled respiration data.

Fig. 5. Power spectral densities of seed pixel, and downsampled respiration and cardiac signals for Subject 1.
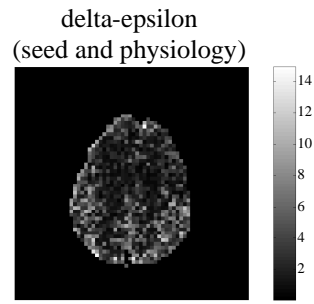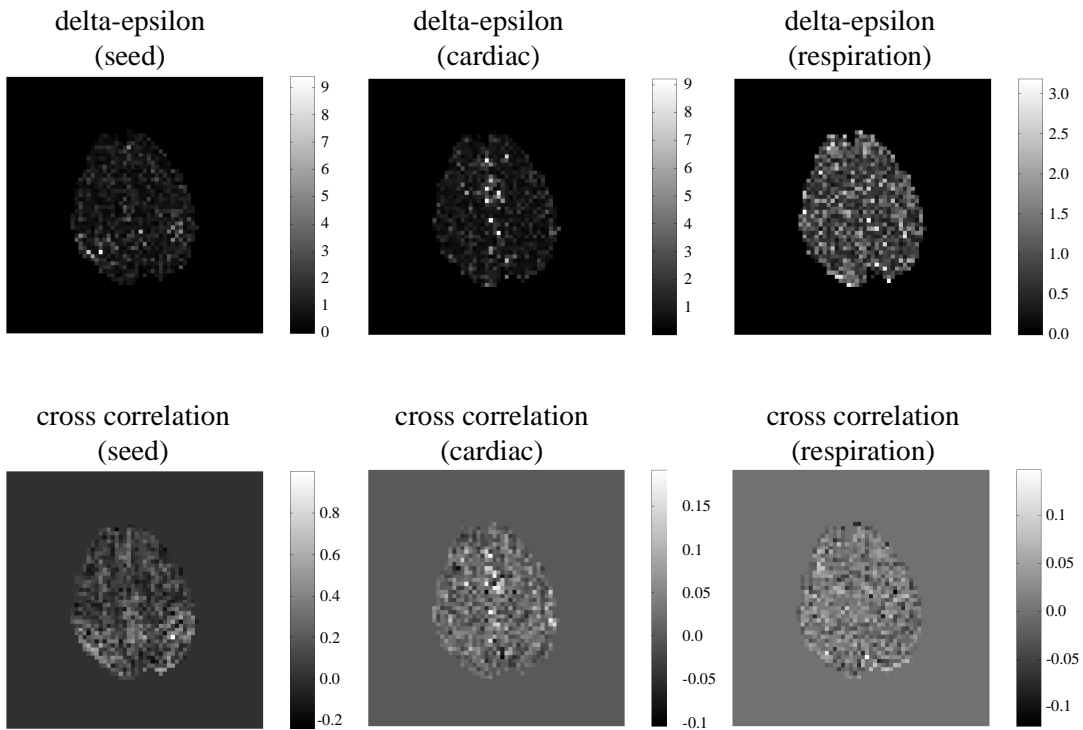
delta-epsilon
(seed and physiology)

Fig. 6. Joint embedding of motor seed pixel and downsampled respiration and cardiac signals for Subject 1.

delta-epsilon
(seed)

delta-epsilon
(cardiac)

delta-epsilon
(respiration)

cross correlation
(seed)

cross correlation
(cardiac)

cross correlation
(respiration)

Fig. 7. de and correlation results using seed pixel, downsampled cardiac data and downsampled respiration data.

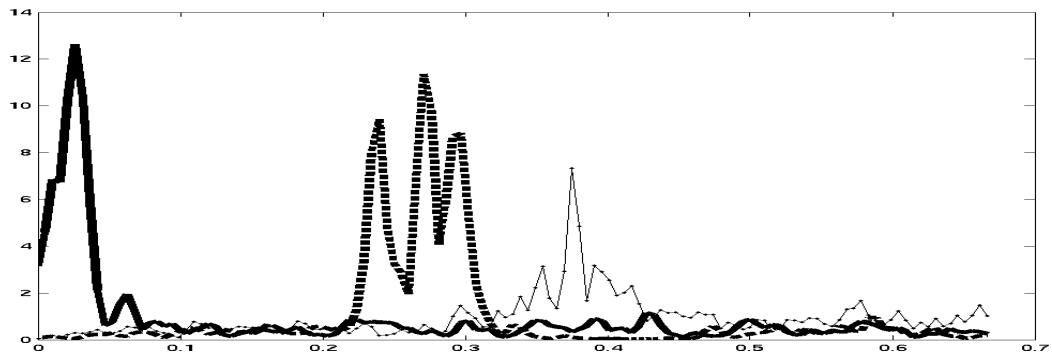Fig. 8. Power spectral densities of seed pixel, and downsampled respiration and cardiac signals for Subject 2.
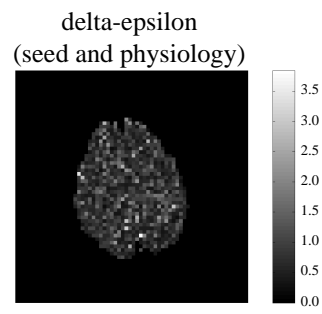
delta-epsilon
(seed and physiology)

Fig. 9. Joint embedding of motor seed pixel and downsampled respiration and cardiac signals for Subject 2.